Methodological re-evaluation of the electrical conductivity of silicate melts

Anne Pommier, Fabrice Gaillard, Mohammed Malki, Michel Pichavant

Revised ms

METHODOLOGICAL RE-EVALUATION OF THE ELECTRICAL CONDUCTIVITY OF SILICATE MELTS

A. Pommier[1*], F. Gaillard[1], M. Malki[2,3] and M. Pichavant[1]

[1] *CNRS/INSU, Université d'Orléans, Université François Rabelais-Tours, Institut des Sciences de la Terre d'Orléans (ISTO), UMR 6113, Campus Géosciences, 1A rue de la Férollerie, 45071 Orléans cedex 2, France*

[2]*CNRS, Conditions Extrêmes et Matériaux : Haute Température et Irradiation (CEMHTI), UPR 3079, 1D avenue de la Recherche Scientifique, 45071 Orléans cedex 2, France*

[3]*Polytech'Orléans-Université d'Orléans. 8, Rue Léonard de Vinci, 45072 Orléans cedex 2, France*

*Corresponding author:
anne.pommier@cnrs-orleans.fr
Tel. +33 2 38 25 53 94
Fax +33 2 38 63 64 88

Abstract

Electrical impedance measurements in laboratory on silicate melts are used to interpret magnetotelluric anomalies. On the basis of two- and four-electrode measurements, we show that the influence of the electrodes of the 2-electrode system on the measured resistivity can be of significant importance for low-resistivity melts and increases with temperature. At 1400°C, the resistivity of very conductive melts measured with two electrodes can reach six times the resistivity value measured with four electrodes. A short-circuit experiment is needed to correct the 2-electrode data. Electrodes contribution is also estimated for samples from other studies, for which the resistance of the electrical cell can be as high as the resistance of the sample. A correction of the resistivity data from the literature is proposed and values of the corresponding Arrhenian parameters are recommended.

Keywords: impedance measurements, resistivity, melts.

INTRODUCTION

The knowledge of the electrical properties of melts is needed for the interpretation of magnetotelluric profiles (Wannamaker et al. 2008; Yoshino et al. 2006; Tarits et al. 2004; Müller and Haak 2004; Roberts and Tyburczy 1999). For example, both magnetotelluric data and electrical measurements in laboratory allowed the identification of partial melt in the asthenosphere below the East Pacific Rise (Yoshino et al. 2006). The information provided by electrical measurements in laboratory is of significant interest to the interpretation of geophysical anomalies, in terms of quantitative constraints placed on potential conductive magma reservoirs (Pommier et al. 2008; Gaillard et al. 2008) and for the elaboration of conductivity models (Xu et al. 2000). Since electrical conductivity (or resistivity) is extremely sensitive to small chemical and physical changes, it represents a subtle probe for studying silicate melts properties under controlled and variable conditions (T, P, composition and fO_2) (Pommier et al. 2008; Gaillard and Iacono Marziano 2005; Gaillard 2004; Tyburczy and Waff 1985, 1983). Several studies have contributed to improve the technique of electrical impedance measurements over the past decades (e.g. Lupotto et al. 1987; Hodge et al. 1976; Bauerle 1969).

Experimental difficulties raised by electrical measurements include the maintenance of a well-constrained electrical cell geometry and the necessity to limit the interactions between the sample and the components of the electrical cell. In addition, the problem of the contribution of the electrical response of the electrodes to the measured resistance can be of non negligible importance (Tyburczy and Waff 1983) and needs to be quantified. Most electrical measurements of natural silicate melts are 2-electrode based, whereas the 4-electrode system is mostly used by the material science community. The resistance of the electrodes ($R_{electrodes}$) is included in the impedance measured by the 2-electrode system, which can affect the electrical response of the sample (effective resistance), particularly for low resistivity melts. It is therefore important to evaluate the contribution of the electrodes in the

experimental conductivity database for silicate melts. Because this problem concern most of the current database of electrical resistivities of natural melts, it also raises a direct implication in the interpretation of magnetotelluric profiles in molten or partially molten regions of the Earth's crust and mantle.

The main goal of this study is to address the influence of the electrode configuration on the measurement of the resistivity of melts in laboratory. We measured the electrical response of three silicate melts (a basalt, a phonolite and a borosilicate) using two different techniques, based on 2- and 4-electrode measurements. Experiments were conducted at 1 bar and in the T range [800-1430°C]. The influence of the electrical response of the electrodes on the 2-electrode data was identified, demonstrating the need for a significant correction of the impedance measurements. Errors on resistivity values of silicate melts due to electrodes contribution were estimated for the investigated samples as well as for samples from other studies. We recommend values of corrected Arrhenian parameters for the calculation of electrical resistivity of natural silicate melts.

EXPERIMENTS

Starting products

The three starting materials were a borosilicate synthetized at the CEMHTI (CNRS-Orléans, France), a phonolite from Mt. Vesuvius (Pommier et al., 2008), and an alkali basalt from the Pu'u' 'O'o volcano (Kilauea). The composition of the Kilauea basalt is close to the typical composition of MORB-type basalts. The samples were chosen for their differences in chemical composition and their geological interest. The starting materials were finely crushed, melted in air at 1400°C during ~1h and quenched into a glass. The composition of the starting glasses is presented in Table 1. For the 2-electrode measurements, the starting materials were melted in air in a Pt crucible and the resulting bubble-free glass was drilled to cylinders (Pommier et al. 2008). For the 4-electrode measurements, the starting materials

were melted in an alumina crucible which was directly used in the electrical conductivity measurements (Simonnet et al.2003).

Basic concepts of complex impedance measurements

Complex impedance measurements allow to study conduction processes by discriminating most of polarization effects observed during a scan in frequency (Bruin and Franklin, 1981). While the electrical resistance of geologic materials has been measured for almost one century (e.g. Volarovich and Tolstoi, 1936), impedance measurements applied to solid electrolytes are more recent (Bauerle, 1969; Tyburczy et Fisler, 1995 and references therein). The interpretation of impedance spectra in terms of transport mechanisms has been widely investigated (Roberts et Tyburczy, 1994; Huebner et Dillenburg, 1995; Roling, 1999).

Impedance spectroscopy consists in recording the electrical impedance of a material at variable frequency. An ac current is delivered between two “current electrodes” and an induced ac voltage drop is measured between two “voltage electrodes”. The complex impedance Z* is deduced, Z*=U*/I*, U* being the voltage drop vector and I* being the current vector (Simonnet et al. 2003). In the 2-electrode system, current and voltage electrodes are conveyed through only two electrodes.

The complex impedance Z* is the sum of a real and an imaginary parts: Z*=R+jX, R being the electrical resistance and X the reactance. Thus, the determination of the electrical resistance of a material consists in extracting the real part of the complex impedance $Z^*_{material}$ (Bagdassarov et al. 2004; Gaillard 2004; Pommier et al. 2008). The electrical resistivity ρ (ohm.m) is deduced from the value of R (ohm) by using the following relation:

$$\rho = G.R \qquad (1)$$

where G is the geometric factor (m) and depends on the dimensions of the material studied and on the distance between electrodes.

Experimental setups

The two experimental setups are presented in Figure 1a. 2-electrode experiments were performed at the ISTO and 4-electrode experiments at the CEMHTI (Orléans, France). All experiments were conducted in air. In both cases, the glass sample was placed in the hot spot of the furnace. Temperature, monitored with a Eurotherm controller, was measured by a type S thermocouple, placed adjacent to the conductivity cell, and is known to within ±2°C. Impedance was measured in response to an AC signal in the 1Hz-1MHz frequency range using an impedance gain/phase analyzer (Solartron 1260, Schlumberger Co.), the voltage amplitude being 0.1 to 0.5V.

In the 2-electrode configuration, the two groups of welded electrodes are connected to a Pt tube (external electrode) and a Pt wire (internal electrode), respectively. The cylindrical geometry of the sample (L from 3.5 to 9mm; OD from 4.5 to 7.5mm and ID=1mm) implies the electrical resistivity to be coaxially measured. An alumina plug prevents the two electrodes from being in contact with each other (Pommier et al. 2008). In the 4-electrode configuration, two Pt sheets serve as current electrodes and two Pt wires measure the voltage drop. The four electrodes are connected separately to the impedance spectrometer and the resistivity is measured between the wires. These Pt foils are totally immersed in the liquid sample contained in the alumina crucible (L>10mm; OD=30mm). As shown in Figure 2, measurements performed at different immersion depths of the electrodes underline that the wetting effect on the measured electrical resistance is negligible for an immersion >5mm (similarly to Gaillard et al. 2008 for very conductive carbonate liquids with high wetting properties). All 4-electrode measurements were performed at an immersion depth of ~8mm. The precision of the immersion depth of the electrodes in the melt is controlled by a mechanical displacement system allowing the depth to be determined with a good precision (0.02mm, Malki and Echegut 2003).

Equivalent electrical circuits are presented in Figure 1b for both configurations. The different components of the electrodes (conductivity cell parts + connecting metallic wires) are associated in series with the effective complex impedance of the sample (Z^*_{sample}). Contrary to the 2-electrode system, the current in the 4-electrode setup is not delivered in the loop of measurement of the potential. As a result, the electrical impedance of the cell is not involved in the measured impedance ($Z^*_{measured}$) and:

$$Z^*_{measured} = Z^*_{sample} + Z''_{induct} \qquad (2)$$

where Z''_{induct} (the imaginary part X of $Z^*_{electrodes}$) represents the inductive effects of the electrodes and was found to be negligible for frequencies <0.1MHz (Simonnet 2004). According to Figure 1b, the impedance measured using a 2-electrode system can be written:

$$Z^*_{measured} = Z^*_{sample} + Z^*_{electrodes} = [R+jX]_{sample} + [R_{Pt\ parts} + Z''_{induct} + (R_{pol} // C_{pol})]_{electrodes} \qquad (3)$$

where $R_{Pt\ parts}$ is the resistance of the Pt tube and Pt wires (Figure 1a) and the association $R_{pol} // C_{pol}$ represents the polarization effects (ionic double-layer). The best method for estimating the electrode contributions is to conduct a short-circuit experiment. Because Pt resistivity is temperature-dependent, short-circuit measurements must be done at temperature. This experiment consists in connecting the two electrodes with a small Pt wire (Figure 1a). Electrical measurements are performed on an empty cell (i.e. without sample) and $Z^*_{short\text{-}circuit} = Z^*_{electrode}$.

Data reduction and calibration

An example of the electrical response of the sample to a scan in frequency is presented in the complex plane (Z', Z") Figure 1c. Graphically, the value of the electrical resistance R corresponds to the intersection of the electrical response with the real axis (i.e. Z"=0). The first part of the response (Z'<R and Z">0) represents the induction effects whereas the second part (Z>R and Z"<0) is attributed to the impedance of the interface between the sample and the electrode (Huebner and Dillenburg 1995).

The determination of the resistivity value ρ requires the determination of the geometric factor G (Eq. 1). For the 4-electrode configuration, G was determined through the calibration of the cell. Calibration was performed using three aqueous KCl solution (0.01, 0.1 and 1M) of known resistivity at room temperature. Standard liquids are generally used for this calibration (Wu and Koch, 1991). The geometric factor of the 4-electrode cell is calculated by measuring the resistance R of the KCl solution and using Eq. 1. Similar values of G were obtained using the different KCl solutions and the geometric factor was found to be 0.039m. For the 2-electrode configuration, the diffusion formalism in a cylinder in which diffusion is coaxial (Crank 1975) showed that G can be written as follows:

$$G = \frac{2\pi L}{\ln(d_{ext}/d_{\text{int}})} \qquad (4)$$

where L is the length of the cylindrical glass sample, d_{ext} is the outer diameter and d_{int} the internal diameter. A constant value of the geometric factor during the experiment is assumed. The uncertainty on ρ due to error propagation of typical uncertainties on R, L, d_{ext} and d_{int} is in the range of 7-12.5% for all melts. Eq. 4 yielded values of G ranging from 0.015 to 0.019m. These values were confirmed by the calibration of the 2-electrode setup cell using KCl solution (1M).

Chemical characterization of the samples

Most glass samples were analyzed after the experiment with a Camebax SX-50 electron microprobe in order to check for interactions between the sample and the cell parts (Pt and alumina). Analyses were conducted at 15 kV, 6 nA, 10 s on peak and 5 s on background. No significant variations in oxides contents were measured in the samples after 2-electrode experiments, in agreement with the observations of other studies using similar electrical cells (Pommier et al. 2008; Gaillard 2004). Iron was found to be present at very low concentrations (<0.5wt%) in the Pt electrodes from the 2-electrode setup. Iron depletion was

thus too small to change significantly the FeO content of the melt. Therefore, we considered that iron loss was of minor importance in this study. Electron microprobe traverses were performed in one sample from the 4-electrode experiments in order to estimate the contamination of the melt by the alumina crucible. Al_2O_3 enrichment was found to affect the melt on a distance <1mm from the Al_2O_3 crucible/melt interface. The melt volume occupied by the immersed electrodes (see Figure 1a) is not spatially concerned by the contaminated melt. A contamination of the whole volume of melt due to convection can be excluded, due to the small value of the Rayleigh number (<200, Jaupart and Tait 1995).

RESULTS

The electrical resistivities of the three investigated melts measured using the 2 and 4 electrode configurations are presented Figure 3. For both configurations, measurements during heating and cooling cycles yielded similar resistivity values, which demonstrates reproducibility (in agreement with Pommier et al. 2008 and Malki and Echegut 2003). The short-circuit experiment was performed with the 2-electrode system, from 800 to 1400°C. A resistance from 1.5 to 2ohm was measured in this T-range, corresponding to the contributions of the electrodes. The configuration adopted for the short-circuit experiment (Figure 1a) does not take into account the resistance of the conductivity cell (Pt tube and inner Pt wire). The resistance of these two Pt parts was calculated on the investigated T range using the known resistivity of Pt and Eq. 1. At 1200°C, the resistance of the Pt tube and inner wire (external and internal electrodes, respectively) represent less than 1% of the resistance of the conductivity cell, the 99% corresponding to the Pt wires (cf Figure 1a). This result underlines the very low contribution of the Pt tube and inner wire to the whole electrode resistance and validates the configuration used for the short-circuit experiment. For all 2-electrode experiments, the resistance of the electrodes was deduced from the measured resistance at each T:

$$R_{sample} = R_{measured} - R_{electrodes} \quad (5)$$

and $$\rho_{sample} = \rho_{corrected} = G.R_{sample} \quad (6)$$

These corrected resistivity values correspond to the “2-electrode corrected” data in Figure 3. The good agreement between 2-electrodes corrected data and 4-electrode data is clearly shown.

The principal result shown in Figure 3 is that the 2-electrode setup used in this study implies a low correction on the measured resistivity values of low-conductive melts (phonolite and basalt), while electrical measurements of high-conductive melts (borosilicate) require either to perform a short-circuit experiment in order to quantify the electrodes contributions or the use of a 4-electrode setup. The correction on 2-electrode data of resistivity values of the basaltic liquid only represents between 2 and 10% of the 4-electrode value and is thus negligible for our coaxial experimental setup. The correction of the 2-electrode data was found to increase with temperature. This can be easily understood since the electrical resistivity of silicate melts decreases with increasing T whereas the resistivity of Pt wires has the opposite behaviour. As shown in Figure 3, the influence of the electrodes affects dramatically the resistivity of the less resistive melt (borosilicate). Indeed, at 1400°C, the resistivity measured with the 2-electrode system (0.05ohm.m) is six times higher than the resistivity value given by the 4-electrode system (0.008ohm.m). A slight but noticeable difference was observed for the data of the phonolitic melt at the highest temperatures: at 1260°C, the resistivity value from the 2-electrode experiment is 0.1ohm.m greater than the value measured in the 4-electrode experiment, corresponding to an error on the 4-electrode value of 37% (=100.(($\rho_{2\text{-electrode}}$-$\rho_{4\text{-electrode}}$)/$\rho_{4\text{-electrode}}$)= 100.(0.1/0.27)).

Measurements were performed at high temperatures on a large interval. The temperature dependence of the electrical response of the investigated samples is shown in Figure 3. All the data can be fitted by an Arrhenian formalism:

$$\sigma = \frac{1}{\rho} = \sigma_0 . \exp\left[\frac{-Ea}{R.T}\right] \qquad (7)$$

with σ the electrical conductivity $(ohm.m)^{-1}$, ρ the electrical resistivity (ohm.m), σ_0 the pre-exponential factor $(ohm.m)^{-1}$, Ea the activation energy (J/mol), R the universal gas constant ($J.mol^{-1}.K^{-1}$) and T the temperature (K). Values of the Arrhenian parameters calculated from 4-electrode measurements are similar to those from 2-electrode corrected measurements and are presented in Table 2.

DISCUSSION

Experiments performed with our 2-electrode setup have underlined the importance of the contributions of the electrodes to the measured resistivities of very low resistivity materials. Comparison was made with other 2-electrode setups from other studies. Setups characteristics are listed in Table 3 and results are presented in Figure 4. The 2-electrode setup used in this study is similar to the setup used in Pommier et al. (2008) (experiments on dry and hydrous tephritic to phonolitic samples), Gaillard and Iacono Marziano (2005) (basalt) and Gaillard (2004) (dry and hydrous rhyolite). Only the sample dimensions slightly changed, modifying the value of G (Eq. 4). The results of the short-circuit experiment performed in this study can be applied to correct the results from the studies mentioned above. Our setup was compared with the techniques presented in Rai and Manghnani (1977) (basalts), Waff and Weill (1975) (trachyte and andesite) and Presnall et al. (1972) (synthetic basalt). The electrical response of the electrodes was estimated using indications given in the different studies. For studies using the loop technique (Rai and Manghnani 1977; Waff and Weill 1975), the resistance of the electrodes corresponds to the sum of the resistances of two metallic wires, calculated as follows:

$$R_{wire} = \rho_{wire} . \frac{l}{S} \qquad (8)$$

with ρ_{wire} the resistivity of the metal (ohm.m) (given in the literature), l the length of the wire (m) and S the cross-section area of the wire (m^2). Regarding the study from Presnall et al. (1972), the resistance of the Pt wires was estimated using Eq. 8 and the resistance of the conductivity cell was calculated using Eq. 1 for the adopted cell geometry (consisting in two Pt crucibles fitted into each other). The sum of both resistances (wires and conductivity cell) corresponds to the resistance of the electrodes. An error of ~20% is assumed on calculations of R_{cell}, due to the lack of information regarding the length of metallic wires or the geometry cell.

The contributions of the electrodes to the measured resistance were estimated using the $R_{measured}/R_{electrodes}$ ratio for this and previous 2-electrode studies, and are presented in Figure 4. The coaxial setup used in our laboratory is efficient for measuring the electrical properties of dry natural silicate melts ($R_{measured}/R_{electrodes}$ >5) and the correction of the electrodes contributions will not significantly modify the measured resistance. In Gaillard (2004) and Pommier et al. (2008), the lowest values of the $R_{measured}/R_{electrodes}$ ratio were obtained for the hydrous rhyolite and hydrous phonolite, respectively, i.e. the most conductive investigated samples. For these samples, $R_{electrodes}$ represents 10 to 40% of R_{sample}, the contribution of the electrodes to the measured resistance increasing with increasing T. The low values of the ratio for the borosilicate from this study and carbonatites from Gaillard et al. (2008) underline the need in conducting short-circuit experiments prior to 2-electrode measurements on very conductive melts. In Gaillard et al. (2008), who performed 4-electrode measurements, a comparison between 4-electrode and 2-electrode data on $(Na,K,Ca_{0.25})_2(CO_3)_2$ at 740°C has shown that electrodes are less conductive than the carbonatite melt. Using a 2-electrode setup similar to the one of the present study implies that the correction of the resistance of the electrodes is not needed for low conductivity values, while it can be critical for high electrical conductivity values.

The critical parameter controlling the electrodes contribution is the dimensions of the metallic wires. According to Eq. 8, the smaller the diameter and the longer the length of a metallic wire, the higher the resistance of the wire and, thus, of the electrodes. This is particularly critical for measurements using the loop technique, since the cell components are two long metallic wires of small diameter (~0.2 to 0.6mm) (Rai and Manghnani 1977; Waff and Weill 1975). The calculation of the sample geometric factor as well as technical considerations regarding these two previous studies is detailed in Waff (1976). The adopted configuration leads to an important contribution of the electrodes to the measured resistance: $R_{electrodes}$ ~5ohm at 1500°C for both studies, while $R_{measured}$ is about 6 to 10ohm at the same temperature. An important effect of the electrodes on the electrical measurements was also calculated for the setup used in Presnall et al. (1972): at 1500°C, the contribution of the electrodes to the measured resistivity represents 30%.

Whatever the 2-electrode setup used, the electrodes contribution decreases with temperature. As a consequence, the correction of 2-electrode measurements is negligible for low conductivity values, such as the conductivity of silicate glasses and solids (e.g. Wanamaker and Duba, 1993; Behrens et al. 2002; Poe et al. 2008; Pommier et al. 2008).

Errors on resistivity values determined using a 2-electrode system can be importance in the interpretation of magnetotelluric anomalies. Laboratory data are needed to interpret high conductive zones detected in the Earth's interior and, particularly, to put constraints on the composition and storage conditions of the melt. Depending on the cell configuration and the length of the connecting metallic wires, measured resistance can be twice as great as the effective resistance of the melt, because of electrodes contributions (Figure 4). A similar change in the electrical response of a silicate melt is observed when increasing the temperature of several hundreds of °C or adding a few wt% of water (Pommier et al. 2008; Gaillard 2004; Tyburczy and Waff 1983, 1985). The identification of the electrodes contributions (Figure 4) in the electrical measurements from other studies allowed the

correction of resistivity values. Based on these corrected resistivities, we have determined Arrhenian laws for each melt. The corresponding Arrhenian parameters, $Ln\sigma_0$ and Ea, are presented in Table 4 and compared to the original published values. These corrected values allow the determination of the electrical resistivity of natural melts on a wide range of chemical composition. The improvement of the interpretation of anomalies detected by geophysical methods is also a matter of electrical measurements in laboratory, including the technical concern of the contributions of the electrodes.

CONCLUSION

Electrical impedance measurements using 2-electrode and 4-electrode systems have been used to discriminate the electrodes contributions of the 2-electrode setup to the measured resistance. The electrodes contributions are dominated by the electrical response of the connecting metallic wires and are successfully eliminated by performing a short-circuit experiment. A correction of the electrodes contribution is possible only if the dimensions (in particular, the length of the metallic wires) are well constrained. The 2-electrode setup used in this study is particularly efficient for measuring the electrical resistivity of low-conductive melts (like most natural silicate melts), whereas the electrode contribution can be important for very conductive melts (like carbonatites). Significant electrode effects, particularly for low-resistive melts and at HT were observed for other 2-electrode setups from previous studies. Errors on the corresponding resistivity values of the melts can be non-negligible in the interpretation of magnetotelluric anomalies. A correction of the database of the resistivity of natural melts was performed and recommended values of Arrhenian parameters were proposed.

ACKNOWLEDGEMENTS

This paper is part of the Ph.D. of A. Pommier. The authors are grateful to T. Orr for providing the Kilauea sample. The authors are grateful to G. Henderson for the editing work and two anonymous reviewers for thorough comments. This study has been supported by the French national agency for research, ANR JC05-42707 (Electrovolc) attributed to F. Gaillard.

REFERENCES CITED

Bagdassarov, N.S., Maumus, J., and Poe, B.T. (2004) Pressure dependence of Tg in silicate glasses from electrical impedance measurements. Physics and Chemistry of Glasses, 45 (3): 197-214.

Bauerle, J.E. (1969) Study of solid electrolyte polarization by a complex admittance method. Journal of Physics and Chemistry of Solids, 30: 2657-2670.

Behrens, H., Kappes, R., and Heitjans, P. (2002) Proton conduction in glass – an impedance and infrared spectroscopic study on hydrous BaSi2O5 glass. Journal of Non-Crystalline Solids, 306 (3): 271-281.

Bruin, H.J., and Franklin, A.D. (1981) An impedance spectroscopy model for electron transfer reactions at an electrode/solid electrolyte interface. *Journal of Electroanalytical Chemistry*, 118, 405-418.

Crank, J. (1975) The Mathematics of Diffusion. 2nd ed., 440 pp., Claredon, Oxford, U.K.

Gaillard, F. (2004) Laboratory measurements of electrical conductivity of hydrous and dry silicic melts under pressure. Earth and Planetary Science Letters, 218 (1–2): 215–228, doi:10.1016/S0012-821X(03)00639-3.

Gaillard, F., and Iacono-Marziano, G. (2005) Electrical conductivity of magma in the course of crystallization controlled by their residual liquid composition. Journal of Geophysical Research, 110, B06204, doi:10.1029/ 2004JB003282.

Gaillard, F., Malki, M., Iacono-Marziano, G., Pichavant, M., and Scaillet, B. (2008) Carbonatite melts and electrical conductivity in the astenosphere. Science, 322: 1363-1365.

Hodge, I. M., Ingram, M. D., and West, A. R. (1976) Impedance and modulus spectroscopy of polycrystalline solid electrolytes. Journal of Electroanalytical Chemistry, 74: 125-143.

Huebner, J. S., and Dillenburg R. G. (1995) Impedance spectra of hot, dry silicate minerals and rock: Qualitative interpretation of spectra. American Mineralogist, 80 (1– 2): 46–64.

Jaupart, C., and Tait, S. (1995) Dynamics of differentiation in magma reservoirs. J Journal of Geophysical Research, 100, B9: 17615-17656.

Lupotto, P., Villa, M., and Ciodelli, G. (1987) Simple methods to improve the performances of network analysers in electrochemical analyses. Journal of Physics E-Scientific Instruments, 20: 634-636.

Malki, M., and Echegut, P. (2003) Electrical conductivity of the CaO-SiO_2 system in the solid and the molten states. Journal of Non-Crystalline Solids, 323: 131-136.

Müller, A., and Haak, V. (2004) 3-D modelling of the deep electrical conductivity of Merapi volcano (Central Java): integrating magnetotellurics, induction vectors and the effects of steep topography. Journal of Volcanological and Geothermal Research, 138: 205-222.

Poe, B.T., Romano, C., Varchi, V., Misiti, V., and Scarlato, P. (2008) Electrical conductivity of a phonotephrite from Mt. Vesuvius: The importance of chemical composition on the electrical conductivity of silicate melts. Chemical Geology, 256 (3-4): 193-202.

Pommier, A., Gaillard, F., Pichavant, M., and Scaillet, B. (2008) Laboratory measurements of electrical conductivities of hydrous and dry Mount Vesuvius melts under pressure. Journal of Geophysical Research, 113, B05205, doi:10.1029/2007JB005269.

Presnall, D.C., Simmons, C.L., and Porath, H. (1972) Changes in electrical conductivity of a synthetic basalt during melting. Journal of Geophysical Research, 77 (29): 5665-5672.

Rai, C.S., and Manghnani, M.H. (1977) Electrical conductivity of basalts to 1550°C. In Magma genesis: Bulletin 96, Oregon Department of Geology and Mineral Industries, edited by H.J.B. Dick, pp 219-232, Portland, OR.

Roberts, J. J., and Tyburczy, J. A. (1994) Frequency dependent electrical properties of minerals and partial-melts. *Surveys in Geophysics*, *15*(2), 239-262.

Roberts, J. J., and Tyburczy, J. A. (1999) Partial-melt electrical conductivity: Influence of melt composition. Journal of Geophysical Research, 104(B4), 7055–7065, doi:10.1029/1998JB900111.

Roling, B. (1999) What do electrical conductivity and electrical modulus spectra tell us about the mechanisms of ion transport processes in melts, glasses, and crystals? *Journal of Non-Crystalline Solids*, *244*(1): 34-43.

Simonnet, C., Phalippou, J., Malki, M., and Grandjean, A. (2003) Electrical conductivity measurements of oxides from molten state to glassy state. Reviews of Scientific Instruments, 74 (5): 2805-2810.

Simonnet, C. (2004) Conductivité électrique des verres et fonts d'oxydes. Effet de l'incorporation de particules RuO2. Thèse du CEA-Valrho, site de Marcoule, pp 176.

Tarits, P., Hautot, S., and Perrier, F. (2004) Water in the mantle : results from electrical conductivity beneath the French Alps. Geophysical Research Letters, 31: L06612, doi:10.1029/2003GL019277.

Tyburczy, J. A., and Fisler, D. K. (1995) Electrical properties of minerals and melts, *Mineral Physics and Crystallography, A Handbook of Physical Constants*, pp.185-208, AGU, Whashington, D.C.

Tyburczy, J. A., and Waff, H. S. (1983) Electrical conductivity of molten basalt and andesite to 25 kilobars pressure: Geophysical significance and implications for charge transport and melt structure. Journal of Geophysical Research, 88(B3): 2413–2430, doi:10.1029/JB088iB03p02413.

Tyburczy, J. A., and Waff, H. S. (1985) High pressure electrical conductivity in naturally occurring silicate liquids. In Point Defects in Minerals, Geophys. Monogr. Ser., vol. 31, edited by R. N. Shock, pp. 78– 87, AGU, Washington, D.C.

Volarovich, M.P. and Tolstoi, D.M. (1936) The simultaneous measurement of viscosity and electrical conductivity of some fused silicates at temperatures up to 1400°C. *Journal of the Society of Glass Technology*, 20: 54-60.

Waff, H. S., and Weill, D. F. (1975) Electrical conductivity of magmatic liquids: effects of temperature, oxygen fugacity and composition. Earth and Planetary Science Letters., 28: 254–260.

Wanamaker, B.J., and Duba A. (1993) Electrical conductivity of polycrystalline olivine containing a silicate glass. Geophysical Research Letters, 20(19): 2107-2110.

Wannamaker, P.E., Hasterok, D.P., Johnston, J.M., Stodt, J.A., Hall, D.B., Sodergren, T.L., Pellerin, L., Maris, V., Doerner, W.M., Groenewold, K.A., and Unsworth, M.J. (2008) Lithospheric dismemberment and magmatic processes of the Great Basin-Colorado Plateau transition, Utah, implied from magnetotellurics. G cubed, 9 (5), doi:10.1029/2007GC001886.

Wu, Y.C., and Koch, W.F. (1991) Absolute determination of electrolytic conductivity for primary standard KCl solutions from 0°C to 50°C. Journal of Solution Chemistry, 20: 391-401.

Xu, Y., Shankland, T.J., Duba, A.G., and Poe, B.T. (2000) Laboratory-based electrical conductivity in the Earth's mantle. Journal of Geophysical Research, 105: 27865-27872.

Yoshino, T., Matsuzaki, T., Yamashita, S., and Katsura, T. (2006) Hydrous olivine unable to account for conductivity anomaly at the top of the astenosphere. Nature, 443: 973-976.

Table 1: Composition of the starting glasses (wt%).

Sample	Borosilicate	Phonolite	Kilauea basalt
SiO_2	50	55.73	49.96
TiO_2	0	0.16	2.41
Al_2O_3	8	21.94	13.24
FeOt	2	1.95	10.88
MnO	0	-	0.13
MgO	0	0.19	7.50
CaO	0	2.87	10.58
Na_2O	22	6.11	2.29
K_2O	0	10.14	0.38
B_2O_3	18	-	-
Total	100	99.09	97.89

Table 2: Values of the Arrhenian parameters.

Sample	Corrected* $Ln\sigma_0$ $(ohm.m)^{-1}$	Uncorrected° $Ln\sigma_0$ $(ohm.m)^{-1}$	Corrected* Ea (kJ/mol)	Uncorrected° Ea (kJ/mol)
Borosilicate	10 *(1.5; 0.1)*	5 *(0.5; 0.1)*	73 *(14; 1)*	31 *(5.5; 2)*
Phonolite	8 *(0.6; 0.1)*	7 *(0.5; 0.2)*	83 *(7; 2)*	79 *(5; 2)*
Kilauea basalt	14 *(1.5; 0)*	13 *(1.5; 0.1)*	177 *(22; 1)*	167 *(17; 2)*

* Corresponds to results from 2-electrode measurements corrected. Similar results with the 4-electrode measurements. See text for details.

° Corresponds to results from 2-electrode measurements.

Relative errors and standard deviations in terms of least unit cited on Ea and $Ln\sigma_0$ values are shown in parentheses *(error; standard deviation).*

Error propagation has been estimated using the error on $Ln\sigma$ and Eq. 7.

$$\Delta Ln\sigma = (1/\sigma).\Delta\sigma = \left|\frac{-1}{2\pi R^2 l}.Ln\frac{de}{di}\right|\Delta R + \left|\frac{-1}{2\pi R l^2}.Ln\frac{de}{di}\right|\Delta l + \left|\frac{1}{2\pi R l}.\frac{1}{de}\right|\Delta de + \left|\frac{-1}{2\pi R l}.\frac{1}{di}\right|\Delta di$$

with R the electrical resistance, l the sample length, de and di its outer and inner diameters, respectively, and ΔX the error on X. ΔR=0.5ohm, and $\Delta de=\Delta di=\Delta l$=0.1mm.

Table 3: Characteristics of the 2-electrode setups used in previous studies.

Source [1]	Technique	External electrode		Internal electrode		Geometric factor of the sample (m)
		Material	Dimensions (mm)*	Material	Dimensions (mm)*	
P et al.08	Cylindrical cell	Pt tube	L : 5-10, D : 5 Thickness : 0.2	Pt wire	L:10-15, D:1	1.4-1.8.10^{-2}
G04	Cylindrical cell	Pt tube	L : 30, D : 6 Thickness : 0.2	Pt wire	L:30, D:1	1.4.10^{-2}
RM77	Loop technique	80%Pt-20%Rh wire	L: 7, D: 0.64	80%Pt-20%Rh wire	L: ~7, D: 0.241	3.6.10^{-2}
WW75 (W76)	Loop technique	80%Pt-20%Rh wire	L: 7, D: 0.64	90%Pt-10%Rh wire	L: ~7, D: 0.241	3.6.10^{-2}
Pr et al.72	Hemispherical cell	Pt hemispherical crucible	L:~20, D:20	Pt hemispherical crucible	L~10: D: 5	~7.10^{-2}

[1] P et al.08 : Pommier et al. (2008), G04 : Gaillard (2004), RM77: Rai and Manghnani (1977), WW75 : Waff and Weill (1975), W76: Waff (1976), Pr et al.72 : Presnall et al. (1972).
*L : length of the electrode (metallic wire or tube or crucible), D : diameter of the electrode.

Table 4: Recommended values of the Arrhenian parameters of silicate melts after the correction of 2-electrode measurements.

Rock type[1]	Source [2]	Original $Ln\sigma_0$ $(ohm.m)^{-1}$	Corrected $Ln\sigma_0$ $(ohm.m)^{-1}$	Original Ea (kJ/mol)	Corrected Ea (kJ/mol)	Correction on ρ at 1300°C (%)[3]
Tephrite[4]	P et al.08	12	13 (2.5)	142	160 (30)	9
Phonotephrite[4]	P et al.08	10	11.5 (0.5)	117	140 (7)	10.5
Hydrous phonotephrite (3.5)	P et al.08	10	10 (0.4)	105	109 (4)	17♦
Phonolite[4]	P et al.08	9.1	10 (0.5)	94	105 (5)	20
Hydrous phonolite (1.1)	P et al.08	7.1	7.8 (1.5)	66	77 (18)	18♦
Hydrous phonolite (5.6)	P et al.08	7.3	7.8 (1.3)	61	72 (17)	20*
Rhyolite[4]	G04	6.7	7.5 (0.5)	70.5	93 (5)	6
Hydrous rhyolite (3)	G04	6.5	6 (0.5)	61	69 (6)	8
Tholeiite	RM77/WW75	12/12	19 (1.5)/22 (2)	135/141	220 (15)/250 (27)	27/40
Alkali olivine basalt	RM77, WW75	6/9.3	16 (2.5)/17 (1.5)	115/104	176 (30)/200 (20)	34/25
Mugearite	RM77	8.3	13 (1.5)	88	148 (18)	27
Trachyte	RM77	5.8	8.8 (0.6)	50	80 (6)	41
Latite	WW75	6.4	10 (1.2)	64	106 (15)	27
Andesite	WW75	6.1	10 (5)	62	116 (7)	23
Synthetic basalt	Pr et al.72	13	18.2 (4.5)	141	213 (55)	5.5

[1] For hydrous melts, the numbers in parentheses correspond to the water content (wt%).
[2] P et al.08 : Pommier et al. (2008), G04 : Gaillard (2004), RM77: Rai and Manghnani (1977), WW75 : Waff and Weill (1975), Pr et al.72 : Presnall et al. (1972).
[3] Corresponds to $100.(1-(\rho_{sample}/\rho_{measured}))$.
[4] Experiments under pressure (0.1-400MPa).
♦ Values at T_{max}=1275°C. * Value at T_{max}=1250°C.
Relative errors on corrected Ea and $Ln\sigma_0$ values are shown in parentheses and have been estimated using the errors on Lnσ and the Arrhenian equation (Eq. 7). See Table 2 for the equation used for error propagation on cylindrical cells (P et al.08, G04). For the wire loop technique and the technique used in Pr et al., 72, the equation used is:

$$\Delta Ln\sigma = \left(\left| \frac{Rcell}{G^2} \right| .\Delta G + \left| \frac{-1}{G} \right| .\Delta Rcell \right) .\sigma$$, with ΔX the error on X, ΔG=10%G (geometric factor), ΔRcell=20%Rcell (cell electrical resistance).

Figure captions

Figure 1: 2-electrode and 4-electrode configurations. a) Drawing of the electrical cells connected to the impedance spectrometer. U and I represent the "voltage" and "current electrodes", respectively. The connection of the 2 electrodes for the short-circuit experiment is represented by the dashed line. Note that the short-circuit experiment is performed on a free-sample cell. b) Equivalent circuit of both cells. With the 2-electrode setup, the resistance of the electrodes is counted in the measured impedance (Z*measured). R_{pol} // C_{pol} represent the polarization effects, $Z"_{induct}$ the inductive effects. See text for details. c) Electrical responses observed in the Nyquist plan (Z', Z") for the Kilauea basalt at 1300°C. The resistance of the sample R(ohm) is obtained for Z" = 0 and represents the real part of the complex impedance (Z'). The higher value of R in the 2-electrode system is attributed to the contribution of the resistance of the two electrodes. The short-circuit measurements underline the contribution of the cell in the 2-electrode configuration.

Figure 2: Changes in electrical resistance as a function of the immersion depth of the 4-electrode system.

Figure 3: Dependence of the electrical resistivity with temperature for the three investigated melts using 2-electrode (triangles) and 4-electrodes (crosses) configurations. Circles correspond to the 2-electrode data without the contribution of the resistivity of the electrodes ("2-electrode corrected"). See text for details. Inset graphs focus on the high temperatures data. Error bars are shown for the 2-electrode corrected data.

Figure 4: Ratio of the measured resistance and the resistance of the electrodes for this study and other studies of the electrical conductivity of silicate melts using 2-electrode measurements. P et al. 08: Pommier et al. (2008), G et al. 08 : Gaillard et al. (2008), GIM 05 : Gaillard and Iacono Marziano (2005), G 04 : Gaillard (2004), RM 77 : Rai and Manghnani (1977), WW 75 : Waff and Weill (1975), Pr et al. 72 : Presnall et al. (1972). Gaillard et al. (2008) performed a 4-electrode study, the data point was a test with a 2-electrode configuration. The lower the ratio, the higher the contribution of the electrodes to the measured resistance.

2-electrode configuration

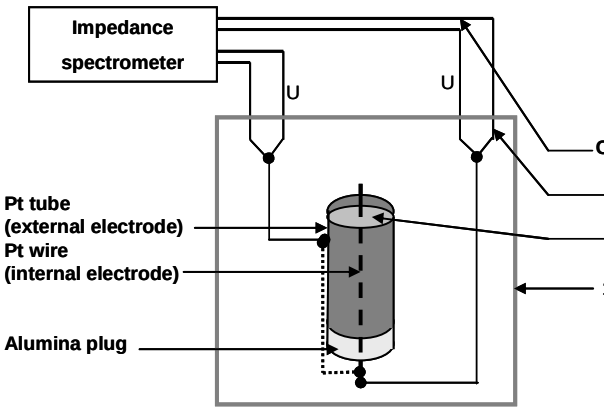

Sample dimensions: *l* = 3.5 to 9mm
od = 4.5 to 7.5mm
id = 1mm

4-electrode configuration

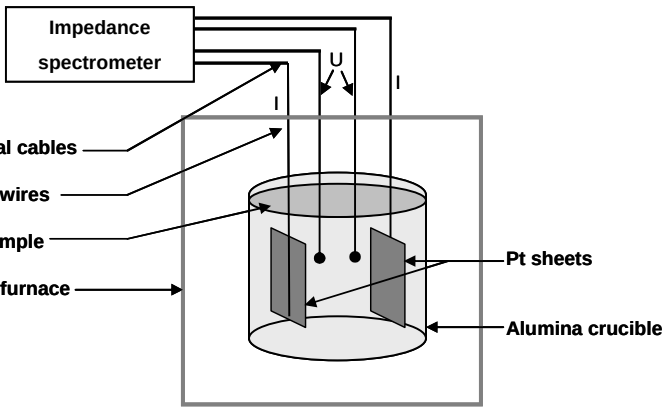

Sample dimensions: *l* ~ 30mm
od = 30mm

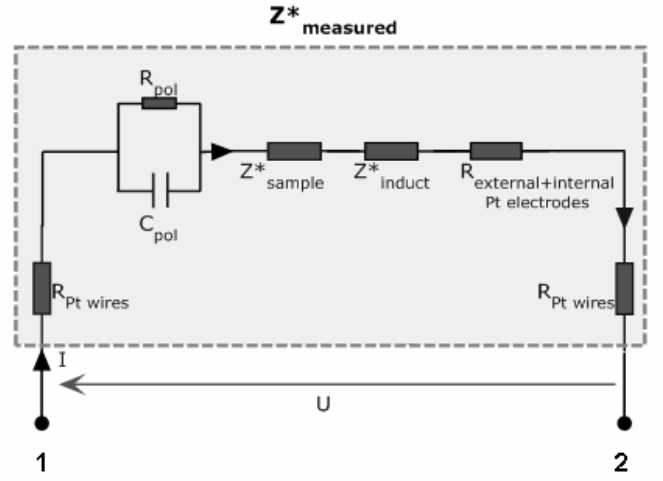

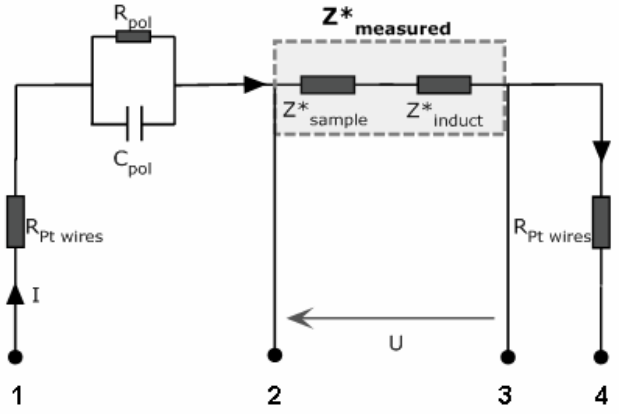

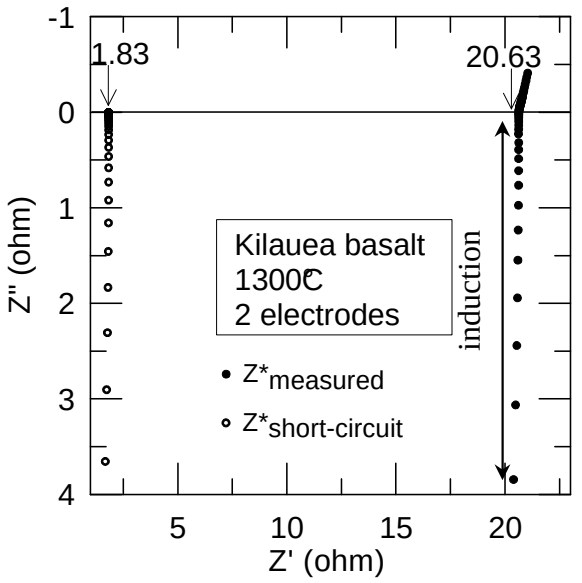

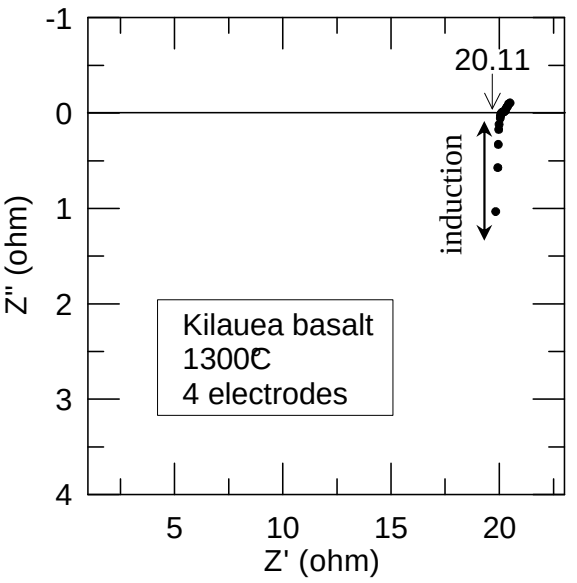

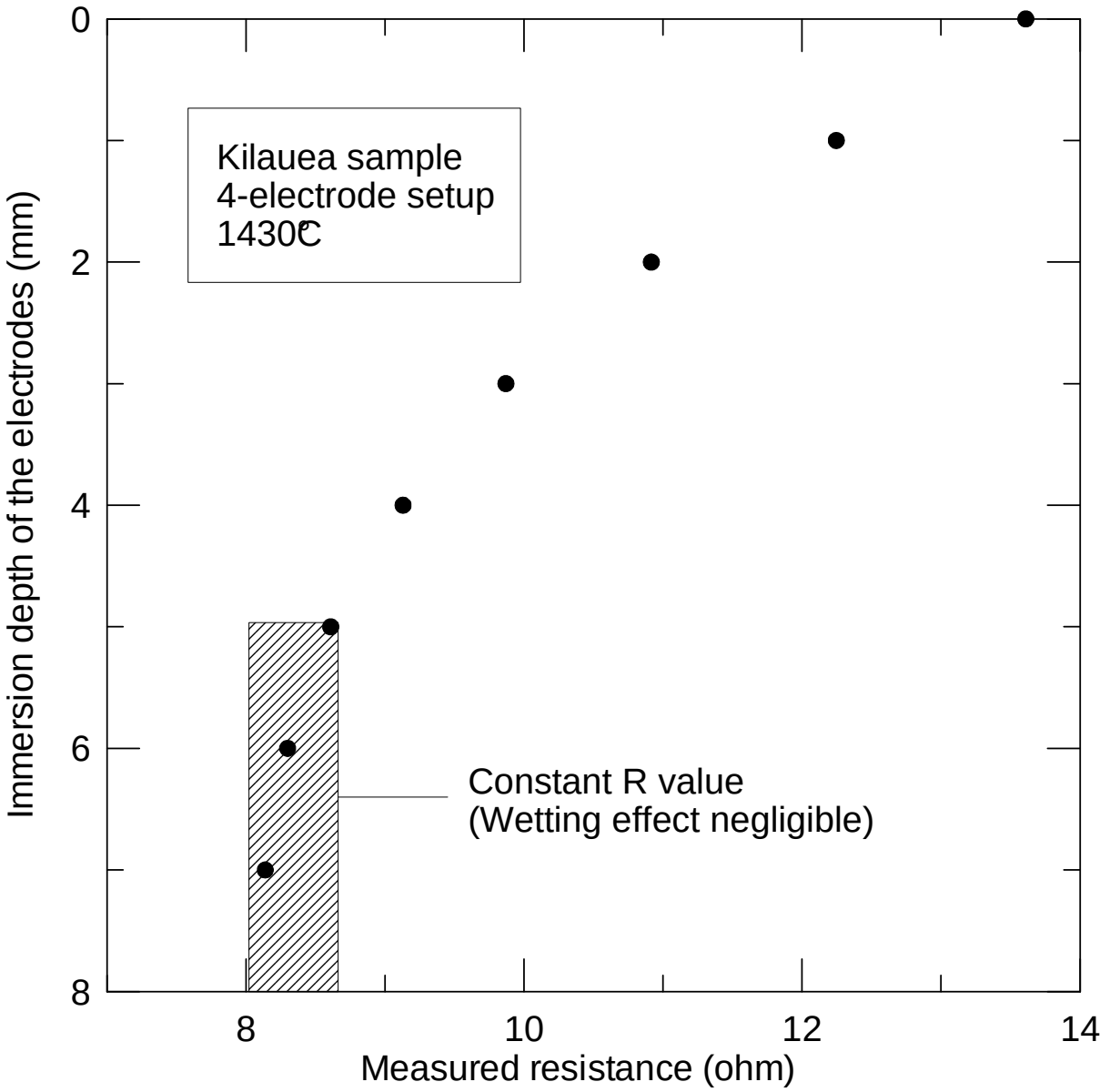
Kilauea sample
4-electrode setup
1430℃
Constant R value
(Wetting effect negligible)
Immersion depth of the electrodes (mm)
Measured resistance (ohm)
0
2
4
6
8
8
10
12
14

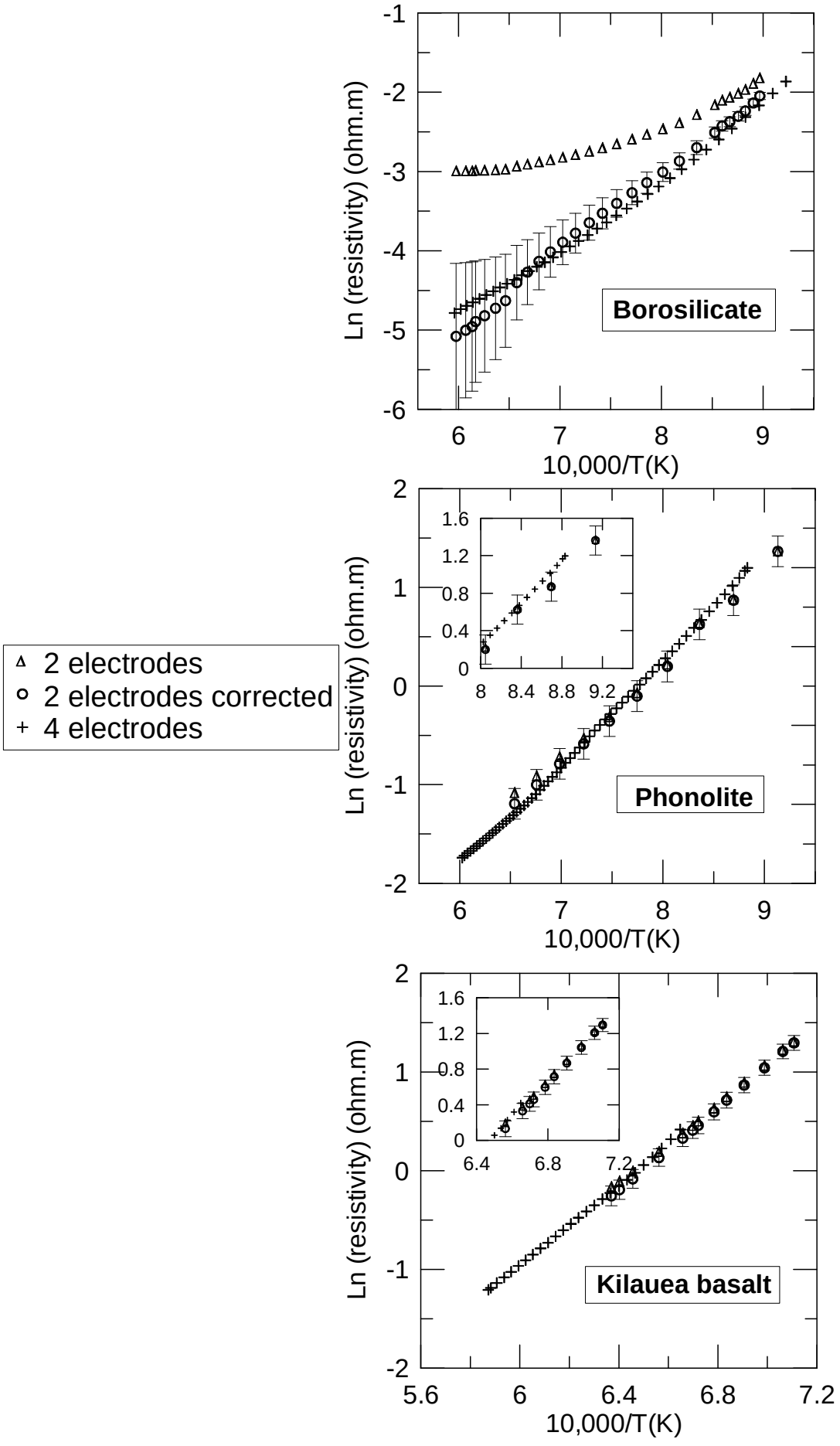
2 electrodes
2 electrodes corrected
4 electrodes
Ln (resistivity) (ohm.m)
10,000/T(K)
Borosilicate
Phonolite
Kilauea basalt

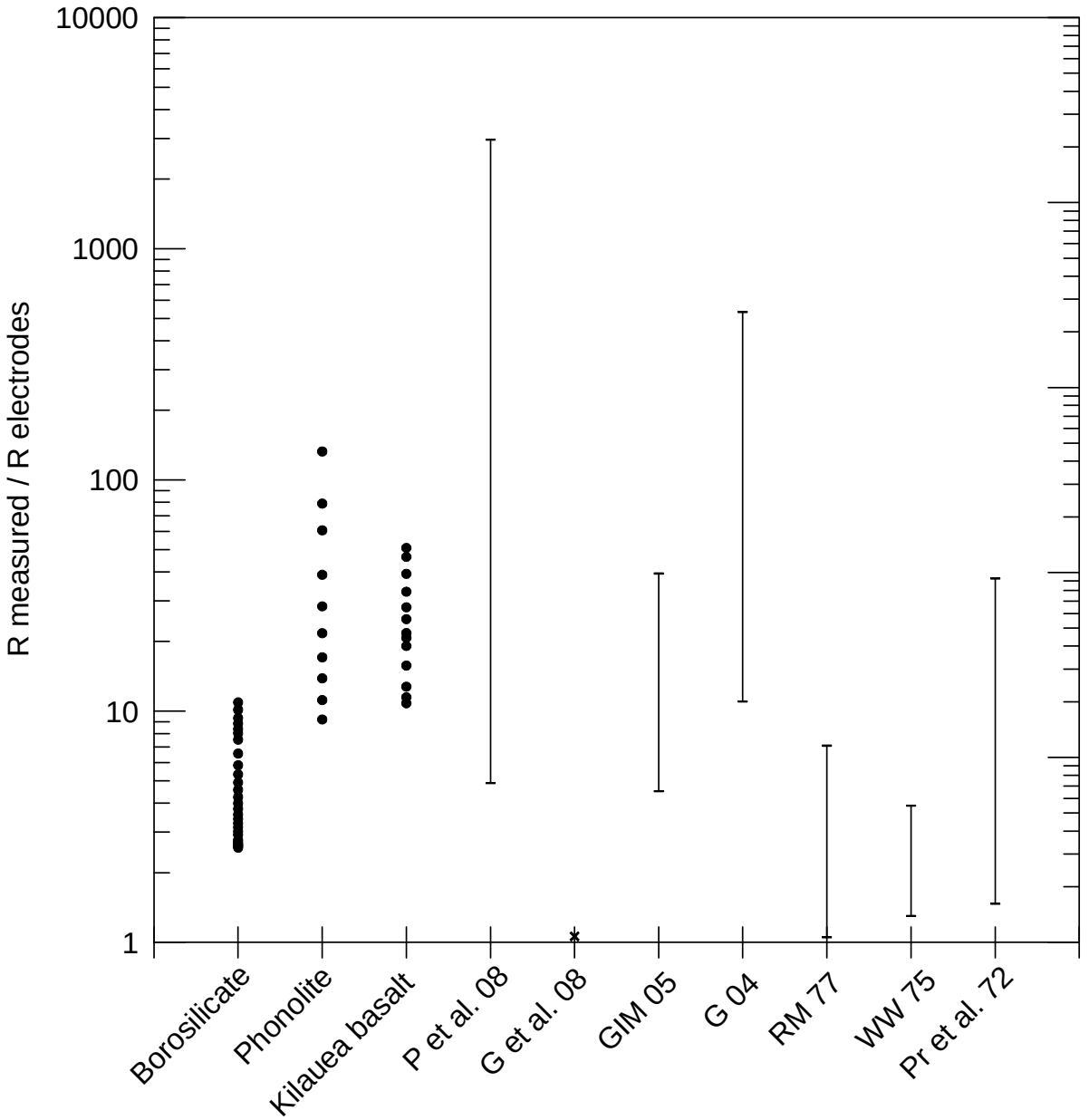
10000
1000
100
10
1
R measured / R electrodes
Borosilicate
Phonolite
Kilauea basalt
P et al. 08
G et al. 08
GIM 05
G 04
RM 77
WW 75
Pr et al. 72